ACS APPLIED MATERIALS & INTERFACES

Research Article

www.acsami.org

Photoisomerization-Induced Manipulation of Single-Electron Tunneling for Novel Si-Based Optical Memory

Ryoma Hayakawa,[†] Kenji Higashiguchi,[‡,§] Kenji Matsuda,*[,‡] Toyohiro Chikyow,[†] and Yutaka Wakayama*[,†,∥]

[†]International Center for Materials Nanoarchitechtonics (WPI-MANA), National Institute for Materials Science, 1-1 Namiki, Tsukuba 305-0044, Japan

[‡]Department of Synthetic Chemistry and Biological Chemistry, Graduate School of Engineering, Kyoto University, Katsura, Nishikyo-ku, Kyoto 615-8510, Japan

[§]PRESTO, Japan Science and Technology Agency, Kawaguchi 332-0012, Japan

[∥]Department of Chemistry and Biochemistry Faculty of Engineering, Kyushu University, 1-1 Namiki, Tsukuba 305-0044, Japan

Supporting Information

ABSTRACT: We demonstrated optical manipulation of single-electron tunneling (SET) by photoisomerization of diarylethene molecules in a metal−insulator−semiconductor (MIS) structure. Stress is placed on the fact that device operation is realized in the practical device configuration of MIS structure and that it is not achieved in structures based on nanogap electrodes and scanning probe techniques. Namely, this is a basic memory device configuration that has the potential for large-scale integration. In our device, the threshold voltage of SET was clearly modulated as a reversible change in the molecular orbital induced by photoisomerization, indicating that diarylethene molecules worked as optically controllable quantum dots. These findings will allow the integration of photonic functionality into current Si-based memory devices, which is a unique feature of organic molecules that is unobtainable with inorganic materials. Our proposed device therefore has enormous potential for providing a breakthrough in Si technology.

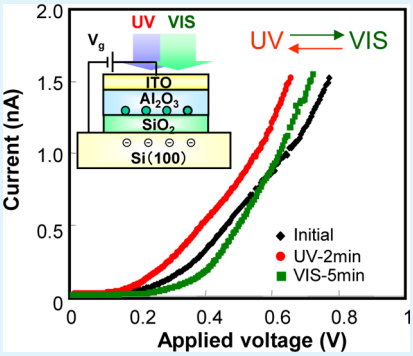

KEYWORDS: *optical manipulation, single-electron tunneling, photochromic quantum dot, metal−insulator−semiconductor*

1. INTRODUCTION

The evolution of complementary metal−oxide−semiconductor (CMOS) devices is now reaching a major turning point owing to the critical limit imposed by increasing large-scale integration and growing power consumption. Single molecular devices such as single molecular transistors and memories have been promising candidates for realizing "beyond CMOS" devices.[1−4] However, the development of such molecular devices is still at the basic research stage, and practical application remains a long way off. The main obstacle is the lack of effective device structures for molecular devices. Device configurations based on nanogap electrodes and scanning probe techniques have poor compatibility with current CMOS technology.[4−8] A realistic solution is to integrate attractive molecular functionality into Si-based devices. For this purpose, we have proposed the adoption of functional organic molecules as quantum dots in a single-electron memory.[9]

Single-electron memory, where Si and Ge nanodots are embedded in a gate insulator, is promising with regard to application to future Si-based memory devices.[10−12] This is because such memory devices make it possible to accumulate carriers in the dots at the single-electron level due to the Coulomb blockade effect. The operating principle allows multilevel operation and ultralow power consumption, which are key issues in relation to future nanoelectronics. Here, we consider organic molecules to be excellent quantum dots compared with their inorganic counterparts. First, the molecules have a uniform size on a nanometer scale, thus achieving quantum dots with a large number density. The number density of the molecules can reach around 10^{13} cm^{-2}, which is two orders of magnitude higher than that of inorganic dots (~10^{11} cm^{-2}).[12,13] Another advantage of the molecules is the tunability of the molecular orbitals.[14−16] Specifically, photochromic molecules, such as diarylethene and azobenzene molecules,[17−19] permit the molecular orbitals to be reversibly changed by light irradiation. That is, the carrier injection for the memory can be manipulated by alternating external triggers, namely, light irradiation and gate voltage. This is a unique feature of organic molecules that makes them very different from inorganic dots.

The factors described above make it possible to integrate unique molecular functions into a single-electron memory, and they provide a potential approach for achieving novel and practical molecular devices. In this paper, we achieved the

Received: August 27, 2013
Accepted: October 7, 2013
Published: October 7, 2013

optical control of single-electron tunneling (SET) via photochromic molecules in a metal−insulator−semiconductor (MIS) structure (Figure 1(a)). A derivative of diarylethene molecules, 1,2-bis(2-methyl-5-(4-biphenyl)-3-thienyl)hexafluoro-cyclopentene, was employed in the form of optically controllable quantum dots in this study. This is because the photoisomerization between the open- and closed-ring isomers of this molecule involves considerable changes in energy levels (Figures 1(b) and 1(c)). Moreover, the photoisomerization is accompanied by a minimal change in molecular geometrical structure, and hence, it can take place even in a solid-state matrix. In the device, the SET threshold voltage was modulated according to a reversible change in the molecular orbital induced by photoisomerization. This finding will allow the integration of photonic functionality into current Si-based memory devices. Our proposed device therefore has enormous potential for providing a breakthrough in Si technology.

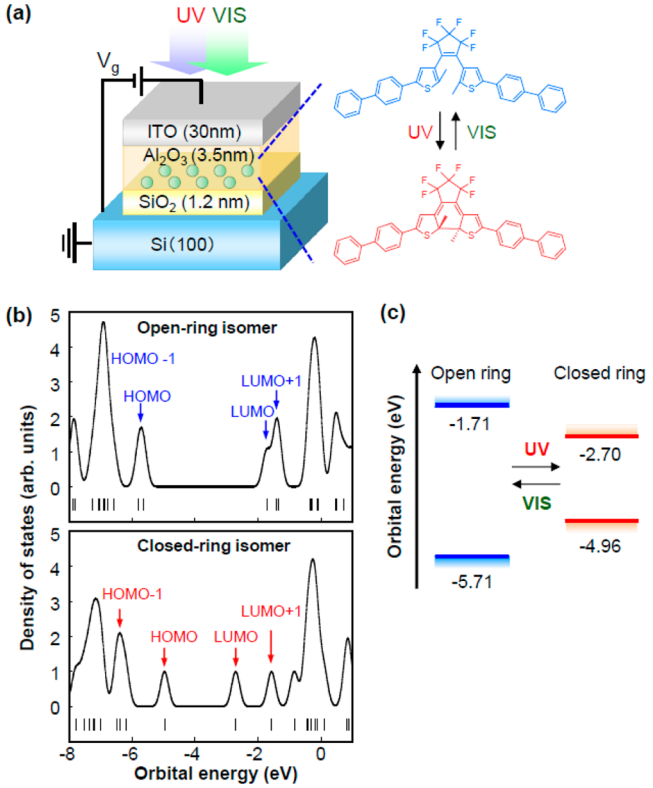

Figure 1. (a) Schematic illustration of a metal−insulator−semiconductor structure with diarylethene molecules, where the molecules are monodispersed in the gate insulator layer. (b) Density of states of diarylethene molecules with open- and closed-ring configurations. Here, the densities of states of the respective isomers were calculated by DFT B3LYP/6-31G(d) using the Gaussian 09 program package. (c) Energy diagram of diarylethene molecules with open- and closed-ring isomers. Here, the values of the HOMO and LUMO levels of the respective isomers were determined from the theoretical calculation in (b).

2. EXPERIMENTAL SECTION

A double-tunnel junction consisting of an ITO/Al_2O_3/diarylethene molecule/SiO_2 multilayer was formed on highly doped p-type Si(100) substrates (<0.01 Ω cm). Here, the Al_2O_3 and SiO_2 thin films served as tunneling barrier layers. First, silicon wafers were cleaned by a chemical treatment known as Shiraki's method,[20] followed by hydrogen termination in diluted HF solution. SiO_2 thin films were grown in a furnace by annealing at 500 °C in an oxygen atmosphere. The wafers were then placed in a combined system composed of an organic deposition chamber and an atomic layer deposition (ALD) reactor. Diarylethene molecules were deposited on the SiO_2 surfaces by thermal evaporation in a vacuum with a background pressure of 5×10^{-7} Pa. The samples were next transferred to the ALD reactor without exposure to air. The Al_2O_3 thin films were formed by introducing trimethyl aluminum and water vapor alternately as precursors. The deposition rate was 1.1 Å/cycle. In this manner, the molecules were completely covered with Al_2O_3 thin films. Finally, transparent ITO electrodes were deposited on top of the Al_2O_3 layers through a shadow mask with a radio frequency magnetron sputtering system to allow light to be irradiated through the electrodes. The transmittances of the ITO layers were estimated to be 50% at 320 nm (UV) and 90% at 600 nm (VIS), where the respective wavelengths correspond to the absorption peaks for open- and closed-ring isomers. The size of the ITO electrodes was 3.1 mm^2.

Current−voltage (I−V) curves were measured using a semiconductor device analyzer (Agilent B1500A) and a four-probe system (Nippon Automatic Control Corporation) in a vacuum at 10^{-3} Pa. The measurement temperature was fixed at 20 K to induce SET via

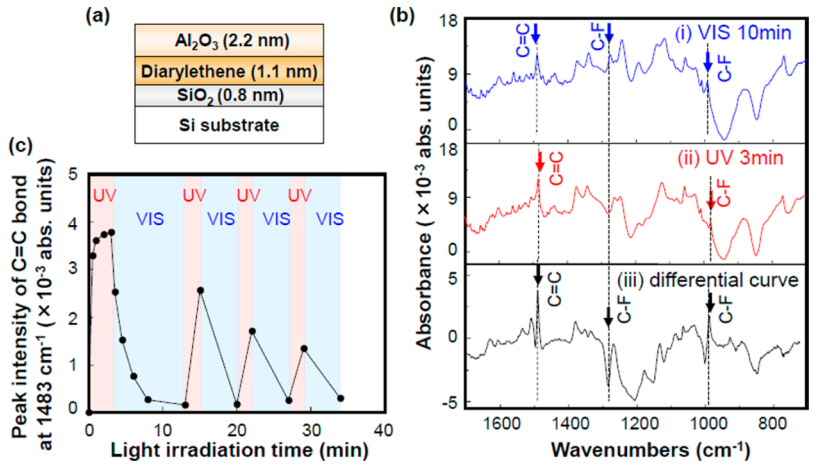

Figure 2. (a) Schematic illustration of an Al_2O_3/diarylethene film/SiO_2/Si multilayer structure for ATR FT-IR measurements. (b) ATR FT-IR spectra of a 45 nm thick diarylethene film with (i) VIS or (ii) UV light irradiation and a difference spectrum. Here, the difference spectrum (iii) was obtained by subtracting spectrum (i) with VIS light for 10 min from spectrum (ii) with UV light for 3 min. The upward peaks are associated with molecular vibration in closed-ring isomers, while the downward peaks are attributed to those in open-ring isomers. (c) Change in peak intensity at 1483 cm^{-1} in differential spectra, corresponding to C═C stretching vibration, against light irradiation time.

diarylethene molecules. A xenon lump (Perkin Elmer Optoelectronics, Cermax lamp) was used as a light source. Here, the UV and VIS lights include wavelengths in the 300−400 nm and 400−700 nm ranges, respectively. The powers of the irradiated lights were estimated to be 11 mW/cm^2 for the UV region and 72 mW/cm^2 for the VIS region with a laser power meter (Ophir Optics, PD300).

To provide clear evidence that the diarylethene molecules undergo photoisomerization even in insulator layers, attenuated total reflection (ATR) Fourier transform infrared (FT-IR) spectroscopy measurements (Thermo scientific, Nicolet iS50) were performed in samples with Al_2O_3/diarylethene thin film/SiO_2/Si multilayer structures. In the experiments, the ATR technique with Ge crystal (Harrick, VariGATR) was adopted to detect molecular vibration signals from diarylethene thin films. The incident angle of the infrared light was fixed at 60°. Here, 1.1 nm thick continuous diarylethene films, where the molecules are not isolated from each other, were sandwiched between Al_2O_3 and SiO_2 layers to detect any change in molecular vibrations accompanied by the photoisomerization in the ATR FT-IR measurements, as illustrated in Figure 2(a). In addition, Al_2O_3 layers were grown at a substrate temperature of as low as 70 °C by the ALD technique to avoid the desorption of the diarylethene thin films from the SiO_2 surfaces (Supporting Information, Figure S1).

3. RESULTS AND DISCUSSION

Figure 2(b) shows ATR FT-IR spectra of diarylethene thin films embedded in the insulator layer with alternating visible (VIS) and ultraviolet (UV) light irradiation. Here, the closed-ring isomer ratio was estimated to be 75% in the UV-light irradiated samples (spectrum (i)). On the other hand, VIS light irradiation for 10 min reduced the ratio to 16% (spectrum (ii)). The derived process in the conversion ratio is shown in the Supporting Information of ref 23. Characteristic vibration peaks in the diarylethene molecule were observed in spectra (i) and (ii), for instance, C═C and C−C stretching vibrations in phenyl and thienyl rings at 1600−1400 cm^{-1} and C−F stretching vibrations in hexafluoro-cyclopentene rings at 1400−800 cm^{-1}.[21,22] Furthermore, the observed molecular vibrations were the same as those in bare diarylethene films (Supporting Information, Figure S3), indicating the fact that there was no change in the molecular structure even after the deposition of Al_2O_3 layers.

The difference spectrum (iii) is shown in Figure 2(b) to clearly identify the differences between open-ring and closed-ring molecular vibrations. Here, the spectrum was obtained by subtracting the spectrum (i) with VIS light from the spectrum (ii) with UV light. We confirmed that some clear differences in molecular vibrations accompanied the photoisomerization. In particular, the three peaks at 1483 cm^{-1} for a thienyl C═C stretching vibration and at 1072 and 977 cm^{-1} for C−F stretching vibrations were found to be greatly changed. In the spectrum, the upward peaks at 1483 and 977 cm^{-1} can be associated with distinctive vibrations in closed-ring isomers, while the downward peak at 1072 cm^{-1} can be attributed to that in open-ring isomers.

To confirm the reversible photoisomerization in the insulator layer, we plotted the change in the peak intensity of the C═C vibration at 1483 cm^{-1} in difference spectra (iii) against a photoirradiation sequence as an indicator of the change from an open-ring to a closed-ring conformation (Figure 2(c)). Prior to the measurement, the samples were irradiated with VIS light for 10 min to initiate the state of the diarylethene molecules into the open-ring isomer. In Figure 2(c), the peak intensity increased immediately after the first UV light irradiation, which shows that closed-ring isomers were dominant. Then, the value saturated at 1 min. Subsequent VIS light irradiation for 5 min restored the peak intensity to the original value as a consequence of the reversible transformation from closed ring to open ring. In this manner, the peak intensity was reversibly changed by alternating UV and VIS light irradiation. These results clearly show that the photoisomerization of diarylethene molecules can be induced even in insulating layers.

It is also noted that the variation in the peak intensity at 1483 cm^{-1} became smaller with repeated photoswitching, although no degradation in photoisomerization appeared in bare diarylethene films (see Supporting Information in ref 23). The deterioration in the photoswitching is probably caused by mechanical fatigue in the molecules accompanied by the repeated conformation change in the insulating layer.

Figure 3(a) shows a current−voltage (I−V) curve and a differential conductance curve, dI/dV, obtained from a double-tunnel junction composed of an ITO/Al_2O_3/diarylethene molecule/SiO_2/Si multilayer measured at 20 K. Here, the 3.2 nm-thick Al_2O_3 and 1.2 nm-thick SiO_2 thin films serve as tunneling barrier layers. The Al_2O_3 layers were formed at 110 °C to improve the insulating properties, although desorption of the diarylethene molecules would occur above 70 °C (Supporting Information, Figure S1). X-ray photoelectron spectroscopy measurements revealed that even though most of the molecules were desorbed during the formation of the Al_2O_3 layer some of the deposited diarylethene molecules remained in the insulator layers (Supporting Information, Figure S4). The density of the molecules was estimated to be about 10^{12} cm^{-2}, and the deposited molecules were fully isolated from each other in the insulator layers. Before the measurement, the sample was irradiated with visible light for 10 min to elevate the open-ring to closed-ring isomer ratio.

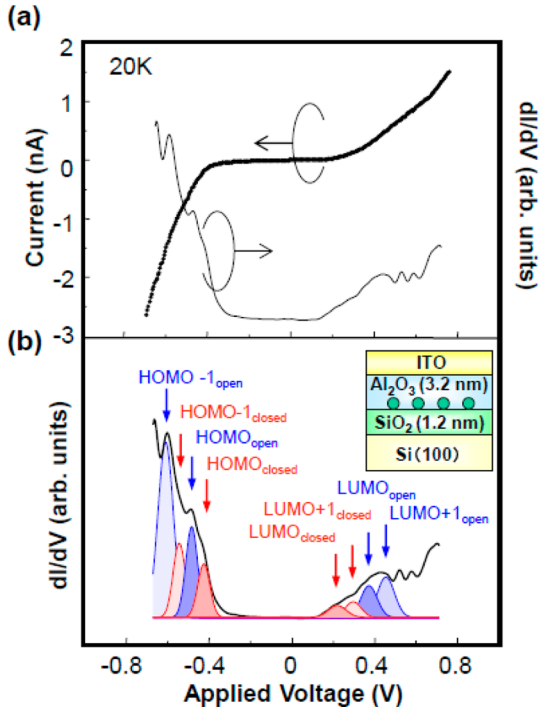

Figure 3. (a) I−V characteristics and the differential conductance (dI/dV). The measurement temperature was 20 K. (b) deconvoluted dI/dV curve by a Gaussian function. Here, the dI/dV curves were deconvoluted into at least eight peaks, which correspond to the energy levels of each isomer.

Multiple Coulomb staircases were seen in the $I-V$ curve (Figure 3(a) and Supporting Information Figure S5(a)), the yield of which was approximately 15%. Meanwhile, no staircases were visible in the samples without molecules (Supporting Information, Figure S5(b)). These results clearly indicate that each diarylethene molecule works as a quantum dot for single-electron tunneling in the double-tunnel junction. Individual molecules are connected electrically in parallel in insulator layers.

Multiple peaks were also observed in the dI/dV curve (Figure 3(a)). In a previous study, we reported that the SET was caused by resonant tunneling through molecular orbitals.[9] This finding confirms that the dI/dV curve reflects the density of states (DOS) of molecules in a gate insulator, which is given by the following equation.

$$I \propto \int_0^{eV} \rho_M(E_F - eV + \varepsilon)\rho_E(E_F + \varepsilon)d\varepsilon \quad (1)$$

$$dI/dV \propto \rho_M(E_F - eV + \varepsilon) \quad (2)$$

where I, ρ_M, ρ_E, and V are the tunneling current, the density of states in the molecules and electrode, and the applied voltage, respectively. The principle described here is the same as that of scanning tunneling spectroscopy (STS).[24,25] As a reference, the DOS of open- and closed-ring isomers of diarylethene molecules were calculated at the B3LYP/6-31G(d) level of density functional theory (Figure 1(b)).[26] Here, the molecular orbitals of respective isomers were labeled as shown in Figure 1(b), although each state was not always composed of a single orbital.

The dI/dV curve in Figure 3(b) was deconvoluted into at least eight peaks by Gaussian fitting, as indicated by the arrows in the figure. On the basis of the calculated molecular orbitals in Figure 1(b), the peaks can be well assigned to the molecular orbitals, including the highest occupied molecular orbital (HOMO) and the lowest unoccupied molecular orbital (LUMO) of the open-ring and closed-ring isomers, respectively. That is, the two isomers coexist although the peak components of the open-ring isomer were more dominant than those of the closed-ring isomer as a result of the initial visible light irradiation prior to the measurement.

The theoretical calculation indicated that the orbital energy of the LUMO level was closed to that of the LUMO+1 level in the open-ring isomer. Meanwhile, these states were completely separated in closed-ring isomers. These variations in the energy levels associated with the photoisomerization were observable in the dI/dV curve. These results reveal that the obtained dI/dV curve exhibits the DOS of diarylethene molecules. The finding provides clear evidence that the carriers can tunnel into the diarylethene molecules from the electrodes through the insulator layers.

The energy levels of molecular orbitals for open- and closed-ring isomers are summarized in Table 1. The values determined by theoretical calculation are also shown in the table for comparison. The relative values of the HOMO and LUMO levels estimated from the dI/dV curves coincided qualitatively with those obtained from the theoretical calculation, although the absolute values are smaller. The observed difference in the absolute values can be attributed to certain causes, e.g., the interaction between molecules and surrounding insulator layers, the Jahn–Teller effect of molecules, and the influence of electric fields.[27,28]

Table 1. HOMO and LUMO Levels of the Diarylethene Molecules with Open- and Closed-Ring Isomers Calculated from the Peak Positions in the dI/dV Curve in Figure 2(b)[a]

	exptl	calcd
$LUMO+1_{open\ ring}$ (eV)	−4.33	−1.40
$LUMO_{open\ ring}$ (eV)	−4.41	−1.71
$LUMO+1_{closed\ ring}$ (eV)	−4.49	−1.56
$LUMO_{closed\ ring}$ (eV)	−4.57	−2.70
$HOMO_{closed\ ring}$ (eV)	−5.23	−4.96
$HOMO_{open\ ring}$ (eV)	−5.29	−5.71
$HOMO\text{-}1_{closed\ ring}$ (eV)	−5.36	−6.39
$HOMO\text{-}1_{open\ ring}$ (eV)	−5.42	−6.91

[a]These values were obtained on the assumption that the Fermi level of the ITO electrode was 4.8 eV. The values determined by a theoretical calculation at the B3LYP/6-31G(d) level are also shown in the table for comparison.

We then examined optical control of the SET. Light irradiation was found to shift the threshold voltages of SET as shown in Figure 4(a). Here, the $I-V$ measurements were

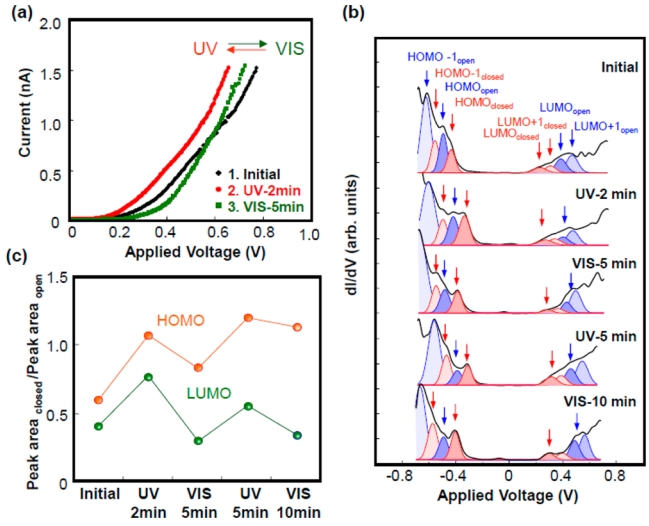

Figure 4. (a) Optical switching of $I-V$ curves and (b) the change in the dI/dV curves induced by the irradiation of UV and VIS lights. Here, the dI/dV curves were deconvoluted by the peaks as assigned in Figure 3(b) using a Gaussian function. The variation in the deconvoluted peak positions was in the ±0.05 V range. (c) Optical switching of the peak ratios between open- and closed-ring isomers induced by alternating the light irradiation. In this calculation, we used the peak areas of the HOMO and LUMO levels of the respective isomers in the dI/dV curve in (b).

conducted at least 5 min after turning off the light to eliminate any influence from the photocurrent and fluctuation in temperature. First, the SET threshold voltage was reduced after UV light irradiation for 2 min. After that, VIS light irradiation for 5 min induced a reversible change to a higher voltage. In this manner, the reversible variation in the threshold voltage was repeatedly observed at several times by alternating the UV and VIS light irradiation (see Supporting Information, Figure S6). No change in threshold voltage in SET was visible without any light irradiation even one day later. These results demonstrate that the diarylethene molecules can work as optically controllable quantum dots in a practical memory device configuration.

The *dI*/*dV* curves after UV and VIS light irradiation, shown in Figure 4(b), were deconvoluted into some peaks and were assigned in a manner similar to those in Figure 3(b). The variation in the deconvoluted peak positions was in the ±0.05 V range, whereas the positions were slightly changed by light irradiation. We assume that the slight shifts in the peak positions were caused by defects in the insulator layers and/or at the interface between the SiO_2 and the Si substrate. A significant point here is that the peak ratio corresponding to the open- and closed-ring isomers could be reversibly changed by the alternate irradiation of UV and VIS light.

Figure 4(c) shows the light-induced change in the ratios of the peak areas between the HOMO and LUMO levels of the respective isomers. The closed-ring to open-ring isomer ratio was elevated by UV light irradiation. The value was in turn reduced by VIS light irradiation; that is, the open-ring isomers became dominant. Here, the disagreement between the peak ratios of the HOMO and LUMO levels can be attributed to the leakage current; i.e., the leakage current overlapped the tunneling current, whose amounts differ with positive and negative voltages. At all events, the reversible change in the SET originated from the photoisomerization of the diarylethene molecules. This finding indicates that the carrier injection into the molecules for memory operation can be controlled by light irradiation as well as gate voltage.

Several similar concepts for optical memories using photochromic molecules have been proposed in the field of organic electronics. For instance, optical memories in crossbar structures with self-assembled monolayers (SAMs) of diarylethene and azobenzene molecules have been reported.[29,30] In these studies, the conductivity of the molecular layers was reversibly controlled by the photoisomerization. Another example is organic transistors with photochromic monolayers.[31,32] Drain current passing through organic semiconductors has been modulated by light irradiation in transistor devices. However, the basic operating principle is always based on the alternating change in the conductivity realized by photoisomerization, that is, operation at a binary variable of "0" or "1". In contrast, our device permits multilevel operation. This is because the carriers can be injected into the different discrete levels in the molecule at distinct threshold voltages, making it possible to accumulate multiple carriers in a single molecule. Namely, the molecules are adopted as quantum dots. These constitute the advantages of our devices for use as conventional photochromism-based devices. Moreover, the threshold voltage can be manipulated by employing light irradiation because the photoisomerization accompanies the changes in the plural molecular orbitals. On this basis, our proposed device represents a prototype device that is "More than Moore", in which photonic functionalities are integrated into Si-based devices.

4. CONCLUSIONS

We demonstrated the optical control of SET via photoisomerization molecules in an MIS structure. The threshold voltage was reversibly manipulated by alternating UV and VIS light irradiation. From an analysis of the *dI*/*dV* curve, we concluded that the change in the SET could be ascribed to the alternation between open- and closed-ring isomers induced by light irradiation. This means that information about the threshold voltage in SET was memorized as a reversible change in the molecular orbitals along with the photoisomerization and reveals that diarylethene molecules work as an optical memory in a practical device structure. These achievements represent unique features of organic molecules that strongly outweigh those of inorganic quantum dots. On the basis of these results, we believe that our proposed device has enormous potential for realizing a breakthrough in Si-based technology.

■ ASSOCIATED CONTENT

Supporting Information

Additional results, including formation process of a multilayer structure, identification of molecular signals with FT-IR, and X-ray photoelectron spectroscopy measurements, are described. This material is available free of charge via the Internet at http://pubs.acs.org.

■ AUTHOR INFORMATION

Corresponding Authors

*E-mail: wakayama.yutaka@nims.go.jp.
*E-mail: kmatsuda@sbchem.kyoto-u.ac.jp.

Author Contributions

All authors contributed equally.

Notes

The authors declare no competing financial interest.

■ ACKNOWLEDGMENTS

This research was supported by the Ministry of Education, Science, Sports, and Culture (MEXT), Grants-in-Aid for Young Scientist (A) 23686051 (2011) and for Science Research on Innovative Areas 23111722 (2011), Kurata grants (2011), and the World Premier International Center (WPI) for Materials Nanoarchitectonics (MANA) of the National Institute for Materials Science (NIMS), Tsukuba, Japan.

■ REFERENCES

(1) Chen, J.; Reed, M. A.; Rawlett, A. M.; Tour, J. M. *Science* **1999**, *286*, 1550−1552.
(2) Park, J.; Pasupathy, A. N.; Goldsmith, J. I.; Chang, C.; Yaish, Y.; Petta, J. R.; Rinkoski, M.; Sethna, J. P.; Abruna, H. D.; McEuen, P. L.; Ralph, D. C. *Nature* **2002**, *417*, 722−725.
(3) Collier, C. P.; Wong, E. W.; Belohradsky, M.; Raymo, F. M.; Stoddart, J. F.; Kuekes, P. J.; Williams, R. S.; Heath, J. R. *Science* **1999**, *285*, 391−394.
(4) Song, H.; Kim, Y.; Jang, Y. H.; Jeong, H.; Reed, M. A.; Lee, T. *Nature* **2009**, *462*, 1039−1043.
(5) Hatzor, A.; Weiss, P. S. *Science* **2001**, *291*, 1019−1020.
(6) Park, H.; Park, J.; Lim, A. K. L.; Anderson, E. H.; Alivisatos, A. P.; McEuen, P. L. *Nature* **2000**, *407*, 57−60.
(7) Yuhsuke, Y.; Shi, Z.; Okazaki, T.; Shinohara, H.; Majima, Y. *Nano Lett.* **2005**, *5*, 1057−1060.
(8) Nakaya, M.; Tsukamoto, S.; Kuwahara, Y.; Aono, M.; Nakayama, T. *Adv. Mater.* **2010**, *22*, 1622−1625.
(9) Hayakawa, R.; Hiroshiba, N.; Chikyow, T.; Wakayama, Y. *Adv. Funct. Mater.* **2011**, *21*, 2933−2937.
(10) Tiwari, S.; Rana, F.; Hanafi, H.; Hartstein, A.; Crabbe, E. F.; Chan, K. *Appl. Phys. Lett.* **1996**, *68*, 1377−1379.
(11) Pace, C.; Crupi, F.; Lombardo, S.; Gerardi, C.; Cocorullo, G. *Appl. Phys. Lett.* **2005**, *87*, 182106−1-182106-3.
(12) Lu, T. Z.; Alexe, M.; Scholz, R.; Talelaev, V.; Zacharias, M. *Appl. Phys. Lett.* **2005**, *87*, 202110−1-202110-3.
(13) Kwon, Y. H.; Park, C. J.; Lee, W. C.; Fu, D. J.; Shon, Y.; Kang, T. W.; Hong, C. Y.; Cho, H. Y.; Wang, K. L. *Appl. Phys. Lett.* **2002**, *80*, 2502−2504.
(14) Lei, S. B.; Deng, K.; Yang, D. L.; Zeng, Q. D.; Wang, C. *J. Phys. Chem. B* **2006**, *110*, 1256−1260.
(15) Sakamoto, Y.; Suzuki, T.; Kobayashi, M.; Gao, Y.; Fukai, Y.; Inoue, Y.; Sato, F.; Tokito, S. *J. Am. Chem. Soc.* **2004**, *126*, 8138−8140.

(16) Zhou, E.; Tajima, K.; Yang, C.; Hashimoto, K. *J. Mater. Chem.* **2010**, *20*, 2362−2368.
(17) Gilat, S. L.; Kawai, S. H.; Lehn, J. M. *J. Chem. Soc., Chem. Commun.* **1993**, 1439−1442.
(18) Luchita, G.; Bondar, M. V.; Yao, S.; Mikhailov, I. A.; Yanez, C. O.; Przhonska, O. V.; Masunov, A. E.; Belfield, K. D. *ACS Appl. Mater. Interfaces* **2011**, *3*, 3559−3567.
(19) Lim, H. S.; Han, J. T.; Kwak, D.; Jin, M.; Cho, K. *J. Am. Chem. Soc.* **2006**, *128*, 14458−14459.
(20) Ishizaka, A.; Shiraki, Y. *J. Electrochem. Soc.* **1986**, *133*, 666−671.
(21) Uchida, K.; Saito, M.; Murakami, A.; Kobayashi, T.; Nakamura, S.; Irie, M. *Chem.—Eur. J.* **2005**, *11*, 534−542.
(22) Stellacci, F.; Bertarelli, C.; Toscano, F.; Gallazzi, M. C.; Zerbi, G. *Chem. Phys. Lett.* **1999**, *302*, 563−570.
(23) Hayakawa, R.; Higashiguchi, K.; Matsuda, K.; Chikyow, T.; Wakayama, Y. *ACS Appl. Mater. Interfaces* **2013**, *5*, 3625−3630.
(24) Uchida, K.; Yamanoi, Y.; Yonezawa, T.; Nishihara, H. *J. Am. Chem. Soc.* **2011**, *133*, 9239−9241.
(25) Nazin, G. V.; Qiu, X. H.; Ho, W. *Science* **2003**, *302*, 77−81.
(26) Frisch, M. J. et al. *Gaussian 09*, Revision B.01; Gaussian, Inc.: Wallingford CT, 2010 (see the Supporting Information).
(27) Yang, Y.; Arias, F.; Echegoyen, L.; Chibante, L. P. F.; Flanagan, S.; Robertson, A.; Wilson, L. J. *J. Am. Chem. Soc.* **1995**, *117*, 7801−7804.
(28) Porath, D.; Levi, Y.; Tarabiah, M.; Millo, O. *Phys. Rev. B* **1997**, *56*, 9829−9833.
(29) Negri, F.; Orlandi, G.; Zerbetto, F. *Chem. Phys. Lett.* **1988**, *144*, 31−37.
(30) Kronemeijer, A. J.; Akkerman, H. B.; Kudernac, T.; Wees, B. J.; Feringa, B. L.; Blom, P. W. M.; de Boer, B. *Adv. Mater.* **2008**, *20*, 1467−1473.
(31) Crivillers, N.; Orgiu, E.; Reinders, F.; Mayor, M.; Samori, P. *Adv. Mater.* **2011**, *23*, 1447−1452.
(32) Yoshida, M.; Suemori, K.; Uemura, S.; Hoshino, S.; Takada, N.; Kodzasa, T.; Kamata, T. *Jpn. J. Appl. Phys.* **2010**, *49*, 04DK09-1−04DK09-4.